



Published in final edited form as:

Int IEEE EMBS Conf Neural Eng. 2021 May ; 2021: 742–745. doi:10.1109/ner49283.2021.9441208.

A Simple Table-Top Technique for Multi-Signal Pseudo-Extracellular Recording

Martin. J. Niemiec,

Biomedical Engineering Department, University of Connecticut, Storrs CT 06268

Martin Han [Senior Member, IEEE]

Biomedical Engineering Department, University of Connecticut, Storrs CT 06268

Abstract

Validation of neural probe performance often includes implantation in live animals, to assess ability to detect and distinguish signals generated by individual neurons. While this method is informative, an effective *in vitro* alternative would streamline device development and improve ethical considerations by reducing the use of animals in the validation of neural recording devices. Here, we describe a simple system using ball electrodes to apply multiple neural waveforms to phosphate buffered saline, which are simultaneously recorded by a microelectrode probe. Using this technique, our neural probe was able to detect and distinguish spikes from multiple units of roughly physiological amplitudes (~100 microvolts peak to peak), indicating promise as an *in vitro* alternative to animal testing for initial validation of neural recording devices.

I. Introduction

Extracellular action potentials (spikes) are known to be the most robust sources of neural encoding. Many electrode designs and materials have been developed to enable detection of spikes *in vivo* [1,2] and *in vitro* [3]. However, *in vivo* validation of new devices for neural recording often requires the use of animals, typically starting with non-survival surgeries. A simple tabletop method involving a physiological solution that can evaluate single- and multi-unit spikes recording capability of new devices would lower development time and cost, and reduce the burden on the animals.

We have previously demonstrated pseudo-extracellular recording of neural waveforms, but only one waveform at a time, and at an amplitude of around one millivolt [4]. Srinivasan et al. demonstrated a similar setup [5], however their system only utilized one source signal. *In vivo*, since there will generally be more than one signal source (neuron) near the probe, a system which can accommodate multiple spatially isolated signals may provide a better simulation of the environment encountered by neural probes.

In this report, we demonstrate a pseudo-extracellular recording system which applies multiple neural waveforms to phosphate buffered saline via ball electrodes. We show that it is capable of recording multiple unique waveforms simultaneously at amplitudes

(martin.han@uconn.edu).

approximating single-unit action potentials *in vivo*, and compare recordings obtained via the system to recordings obtained from cat sensorimotor cortex.

II. Methods

A. Electrode Placement and Positioning

Two ball electrodes were positioned 1cm apart above a beaker containing roughly 250 mL of phosphate buffered saline (PBS) mounted on a scissor jack (Figure 1). A customized multisite silicon-based two-shank probe was affixed to a stereotaxis platform and moved toward the ball electrodes until the shanks of the probe were midway between the two ball electrodes. The probes have previously been extensively validated in chronic *in vivo* experiments [4][6–11]. Considering this distance “zero”, the probe was then retracted using the stereotaxis platform to a distance of 1 cm. A large platinum counter electrode was also positioned in the PBS. The beaker of PBS was then raised using the scissor jack until all electrodes were fully submerged. The entire system was housed within a Faraday cage.

B. Pseudo-Extracellular Recording

Two source waveforms (previously collected from cat sensorimotor cortex, high-pass filtered, and converted to .wav format using a MATLAB script) were used [12]. Two computers were used, each playing a different source file via Windows Media Player (Microsoft, Inc. Redmond, WA, USA) at maximum audio output volume. Each signal was fed through a Plexon Headstage Tester Unit (HTU) to attenuate voltage output to a roughly physiological level, then directed through a ball electrode (CONMED, Inc., Utica, NY, USA) into PBS. The signals were then detected by the silicon probe, amplified, high-pass filtered and recorded using a Plexon OmniPlex® Neural Data Acquisition System (Plexon Inc., Dallas, TX, USA) at a sampling frequency of 40 kHz, with gain and threshold settings automatically configured for each channel in PlexControl. The counter electrode and both Plexon Headstage Tester Units were connected to the Plexon amplifier’s auxiliary ground. Source signals were collected directly from the 3.5 millimeter audio jack and routed to the Headstage Tester Unit. The ground channel of the audio jack was not used. A male Omnetics connector (Omnetics Connector Corporation, Minneapolis, MN, USA) with exposed wires on the opposite end was attached to the HTU and used to transmit the attenuated source signal to the ball electrodes in PBS at room temperature (~25°C).

Audio files were generated from two original source datasets: channels 48 and 35 of what will be referred to as “Subject #8” and “Subject #10”, respectively. Each audio file was first played individually via its respective ball electrode, then both audio files were played simultaneously. At least two minutes of data were recorded for each combination, as well as several seconds of noise for reference. Around 30 microvolts of periodic noise were still detectable inside the Faraday cage, placing a lower limit on detectable signals. Better shielding may allow the system to detect signals of lower amplitude than the ~100 microvolts recorded here.

C. Analysis

All data were analyzed using Plexon Offline Sorter™. For pseudo-extracellular recordings, one channel was analyzed, corresponding to one electrode site on the microelectrode probe. A 150 Hz low-cut filter was applied prior to spike detection to avoid miscategorizing features of the periodic noise as action potentials. Waveforms were aligned by global minimum for negative-going spikes (Subject #10) and global maximum for positive-going spikes (Subject #8), to ensure that the leading edge of the spike was not cut off by the software. Once aligned, waveforms were sorted into units using valley-seeking method with Parzen multiplier 1.15. A few highly irregular waveforms were present after sorting and were invalidated.

In addition to the pseudo-extracellular recordings collected, the original extracellular recordings used to generate the audio files were analyzed using the same methods. As a way to quantitatively compare the pseudo-extracellular recordings to their original recording counterparts, average spikes per minute were calculated by dividing the total number of spikes identified as belonging to a particular unit by the total length of the recording.

III. RESULTS

The source datasets used were specifically selected because each featured a single, distinctive unit. Figure 2's top row shows the high-pass filtered waveforms of the source file (left) and as recorded by our system (right), illustrating spikes over the baseline noise levels. Figure 2's bottom row shows sorted spikes, with Subject #8's distinctive unit shown on the left. If the system was working properly, a unit of the same shape was expected to appear in data collected during pseudo-extracellular recording. Indeed, the unit present after sorting the pseudo-extracellular recording data (right) was nearly identical in shape to the distinctive unit of Subject #8 (left).

While Subject #8's distinctive unit was positive-going, with a positive peak preceding a negative peak, Subject #10's unit was negative-going, making the shapes of the two units easily distinguishable. Figure 3 shows the waveforms (top row) and sorted spikes (bottom row) from the source data and pseudo-extracellular recording for Subject #10. Here, too, the shape of the source waveform's distinctive unit was captured by our system, though some distortion appeared to occur on the tail end of the waveform (Figure 3, bottom right). For both Figures 2 and 3, the waveforms of Subject #8 and Subject #10 were applied to the electrolyte individually, one after the other, to characterize the shape of each distinctive unit.

Figure 4 shows high-pass filtered waveforms (top row) and spike-sorted data (bottom row) from recordings during which both waveforms (Subject #8 and Subject #10) were applied to PBS simultaneously. From left to right, the bottom row shows the sorted data for both units at once, as it appeared in the sorting software, and each unit on its own to better illustrate its shape. Even though both waveforms were being applied to PBS at once, the system was able to identify spikes belonging to Subject #8 and Subject #10's waveforms and sort them into separate units (Figure 4, bottom row).

Subject #8 and #10's pseudo-extracellular recording units had amplitudes of roughly 100 microvolts peak to peak when played both individually (Figures 2 and 3) and together (Figure 4). Both pseudo-extracellular recording units were about half the amplitude of the corresponding unit of the original source waveforms (Figures 2 and 3, left columns). The fact that the system was able to record signals with half the amplitude of the original extracellular action potentials bodes well for its sensitivity and capability in characterizing microelectrode functionality.

The average number of spikes per minute (firing rate) for Subject #8's characteristic unit were calculated to be 759, 686, and 604 in the original file, single-signal recording, and combination recording, respectively. For Subject #10, the average spikes per minute were calculated to be 592, 611, and 612, respectively.

IV. Discussion

While there was precedent for pseudo-extracellular recordings of individual signals in PBS [4,5], it was not known how the signals would be affected during a recording in which both are played simultaneously: would the system perceive the signals as two waveforms of proper shape, or one misshapen waveform? The ability to distinguish multiple units is crucial *in vivo*, and our system was indeed able to separate the two waveforms, faithfully representing each unit's distinctive shape even when both signals were applied simultaneously (Figure 4). There did, however, appear to be some distortion, particularly evident in the tail ends of some of Subject #10's waveforms. The cause of this distortion is not known, though it could potentially be a result of the high volumes at which the audio files were played.

A decrease in detected spikes per minute was expected, as increasing amounts of noise combined with reduced spike amplitudes could affect recording quality. This pattern held true for Subject #8 but did not for Subject #10. This could potentially be explained by the profile of the periodic noise present in the experimental setup. A small (~30 microvolt) noise signal was present (likely a result of ambient 60 Hz signals) which occasionally registered as a negative-going spike. Since Subject #10 is also negative going, but Subject #8 is not, increased levels of this noise may have caused more waveforms to have a profile similar to Subject #10's rather than Subject #8's. However, since the noise was relatively small compared to the amplitude of the recorded spikes, this seems unlikely to present a large enough effect to fully explain the pattern shown by Subject #10. Further investigation is needed to determine the cause and severity of this effect. Different sorting parameters may also improve results—manual thresholding, better filtering, or a different sort style might help to improve spike clustering. Additionally, an improved Faraday cage would prove useful in improving the quality of recorded signals, as well as in increasing the sensitivity of future experiments.

All experiments were performed using PBS at room temperature. Because electrical conductivity of solutions tends to increase with temperature, as a result of increased mobility of ions in solution among other factors [13], it is possible that the system could perform slightly differently at physiological temperatures (~37°C rather than ~25°C), perhaps being

slightly more sensitive as a result of increased conductivity. Future experiments could be performed using a solution maintained at 37°C for increasingly realistic recreation of *in vivo* conditions. The size and shape of the beaker containing the PBS appear unlikely to significantly impact results, as no immediately obvious changes to the signal were visible when the distance from the ball electrode to the probe was changed. But, because the probe used features “window”-type electrodes, which are restricted to one side of the probe shank, alignment of the probe with respect to the signal source may have an effect on the resulting signal. Initial results from ongoing experiments indicate that probe alignment vs. the signal source does indeed affect the amplitude and signal-to-noise ratio of the recorded signal, which will be expanded upon in future work.

With this experiment, we have shown that it is possible to use pseudo-extracellular recording with ball electrodes in phosphate buffered saline to adequately simulate the kinds of signals a neural probe might encounter in the *in vivo* environment. Notably, we were able to detect voltages which were of amplitudes similar to those generated by individual neurons *in vivo*, a significant improvement over our previous pseudo-extracellular recording system. We also showed that it is possible to apply multiple signals to the electrolyte in a way that mimics the activity of multiple distinct neurons, another step closer to an accurate *in vitro* approximation of the *in vivo* environment.

With the use of stereo audio files, the experimental setup used here could be modified to apply up to four unique signals to the electrolyte, adding further rigor with which a probe’s performance can be assessed. Different placements of the ball electrodes could be also be employed: varying distance to the microelectrodes, or placing them behind or to the side, to simulate the distribution of neurons *in vivo*. Furthermore, the addition of source signal monitoring, *i.e.* recording the waveform applied to the ball electrode while simultaneously recording from the microelectrode probe, could allow for experiments similar to evoked-response studies to be performed *in vitro*.

The breadth of experiments which can be performed by this tabletop system has only begun to be realized; as such, we feel that this technique could be a very valuable tool for researchers in the neural engineering field, offering a simple and effective way to evaluate the effectiveness of new neural recording devices before implantation *in vivo*. Importantly, such a system not only offers improvements to administrative, budgetary, and temporal efficiency, but also allays ethical concerns associated with acute, non-survival animal studies presently used, lending it the potential to become quite widely adopted.

Acknowledgments

This work was supported by NIH grants R01DC014044 and R24NS086603 (MH).

References

- [1]. Liu X, McCreery DB, Bullara LA, & Agnew WF “Evaluation of the stability of intracortical microelectrode arrays.” *IEEE Transactions on Neural Systems and Rehabilitation Engineering* 14.1 (2006): 91–100. [PubMed: 16562636]

- [2]. Liu X, McCreery DB, Carter RR, Bullara LA, Yuen TG, and Agnew WF “Stability of the interface between neural tissue and chronically implanted intracortical microelectrodes.” *IEEE transactions on rehabilitation engineering* 7.3 (1999): 315–326. [PubMed: 10498377]
- [3]. Soussou W, Gholmieh G, Han M, Ahuja A, Song D, Hsiao MC, Wang Z, Tanguay AR and Berger TW “Mapping spatio-temporal electrophysiological activity in hippocampal slices with conformal planar multi-electrode arrays.” *Advances in Network Electrophysiology*. Springer, Boston, MA, 2006. 127–152.
- [4]. Nolta NF, Ghelich P, Ersöz A and Han M “Fabrication and modeling of recessed traces for silicon-based neural microelectrodes.” *Journal of neural engineering* 17.5 (2020): 056003. [PubMed: 32947274]
- [5]. Srinivasan A, Tipton J, Tahilramani M, Kharbouch A, Gaupp E, Song C, Venkataraman P, Falcone J, Lacour SP, Stanley GB and English AW “A regenerative microchannel device for recording multiple single-unit action potentials in awake, ambulatory animals.” *European Journal of Neuroscience* 43.3 (2016): 474–485.
- [6]. Pikov V, McCreery DB and Han M (2020). “Intraspinal Stimulation with Silicon-Based 3D Microelectrode Array for Bladder Voiding in Cats.” *Journal of Neural Engineering*.
- [7]. McCreery DB, Yadav K, Han M (2018). “Responses of neurons in the feline inferior colliculus to modulated electrical stimuli applied on and within the ventral cochlear nucleus; Implications for an advanced auditory brainstem implant.” *Hearing Research* (363): 85–97. 10.1016/j.heares.2018.03.009
- [8]. McCreery DB, Han M, Pikov V, and Pannu S (2013). “Encoding of the amplitude modulation of pulsatile electrical stimulation in the feline cochlear nucleus by neurons in the inferior colliculus; Effects of stimulus pulse rate.” *Journal of Neural Engineering*. 10 (17): 056010. [PubMed: 23928683]
- [9]. Han M and McCreery DB (2008). “A New Chronic Neural Probe with Electroplated Iridium Oxide Electrodes.” *Proc Ann Int Conf of the IEEE Eng Med Biol Soc*, Vancouver, Canada. 4220–4221.
- [10]. Han M and McCreery DB (2021). “Future Development: Penetrating Multisite Microelectrodes as Cochlear Nucleus Implant,” in “Auditory Brainstem Implants.” Wilkinson EP and Schwartz MS. Thieme Medical Publishers. eISBN 978-1-62623-827-5
- [11]. Ghelich P, Nolta N, and Han M (2021), “Unprotected Sidewalls in Implantable Silicon Devices and Conformal Coating as a Solution” *npj Materials Degradation*. DOI: 10.1038/s41529-021-00154-9.
- [12]. Nambiar A, Nolta N, and Han M (2019). “3D Reconstruction of the Intracortical Volume Around a Hybrid Microelectrode Array.” *Frontiers in Neuroscience* 13 (393). doi: 10.3389/fnins.2019.00393.
- [13]. Barron JJ, & Ashton C (2005). “The effect of temperature on conductivity measurement”. *TSP*, 7(3), 1–5.

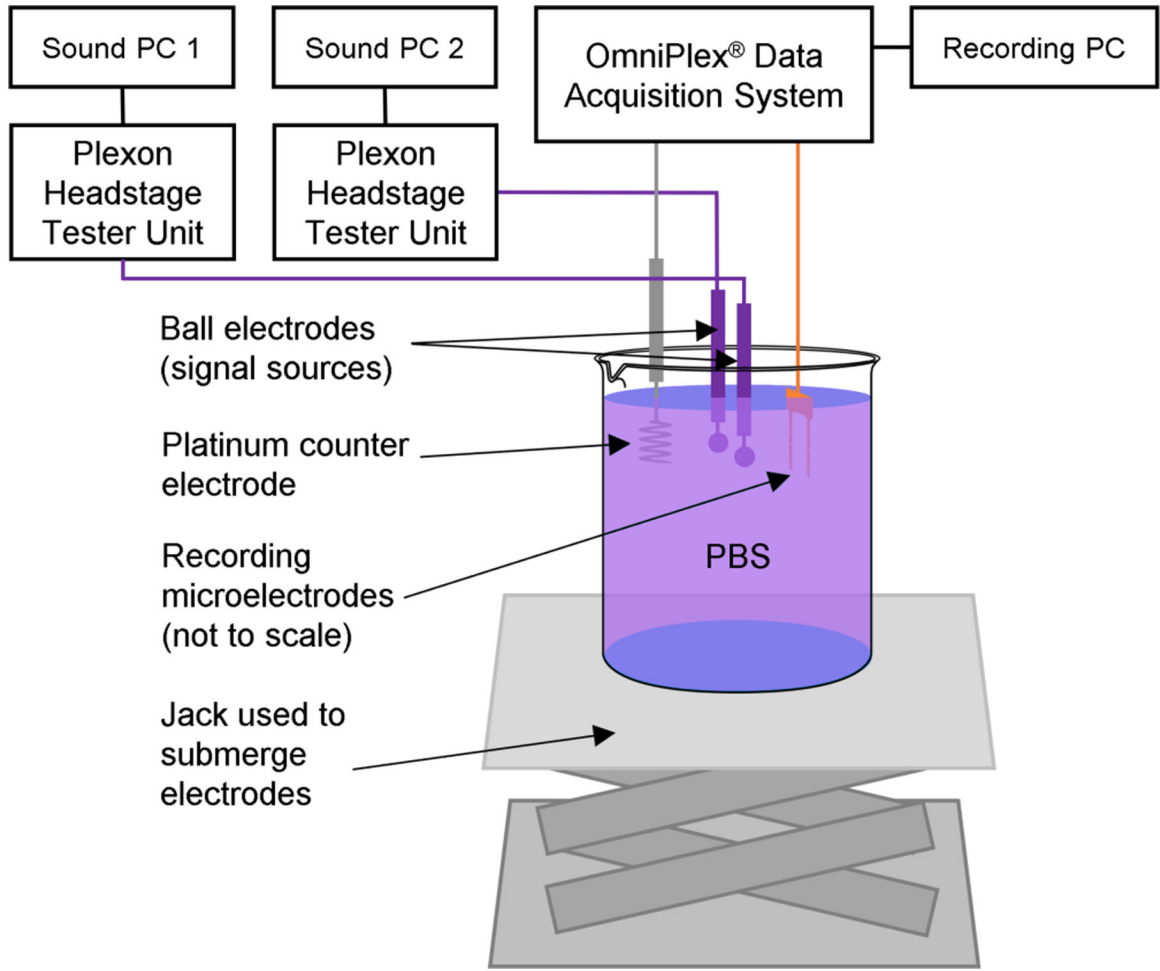


Figure 1: Experimental setup for multi-signal pseudo-extracellular recording. Two ball electrodes were separately connected to two PCs, each playing unique sound files of previously recorded neural signals. A multisite silicon probe was used to record electrical potentials generated by the ball electrodes while the sound files were played. A scissor jack was used to submerge the electrodes without moving them relative to each other by raising a beaker of PBS to meet them. Figure adapted from Nolte *et al.* [4].

Subject #8: extracellular recording vs. pseudo-extracellular recording

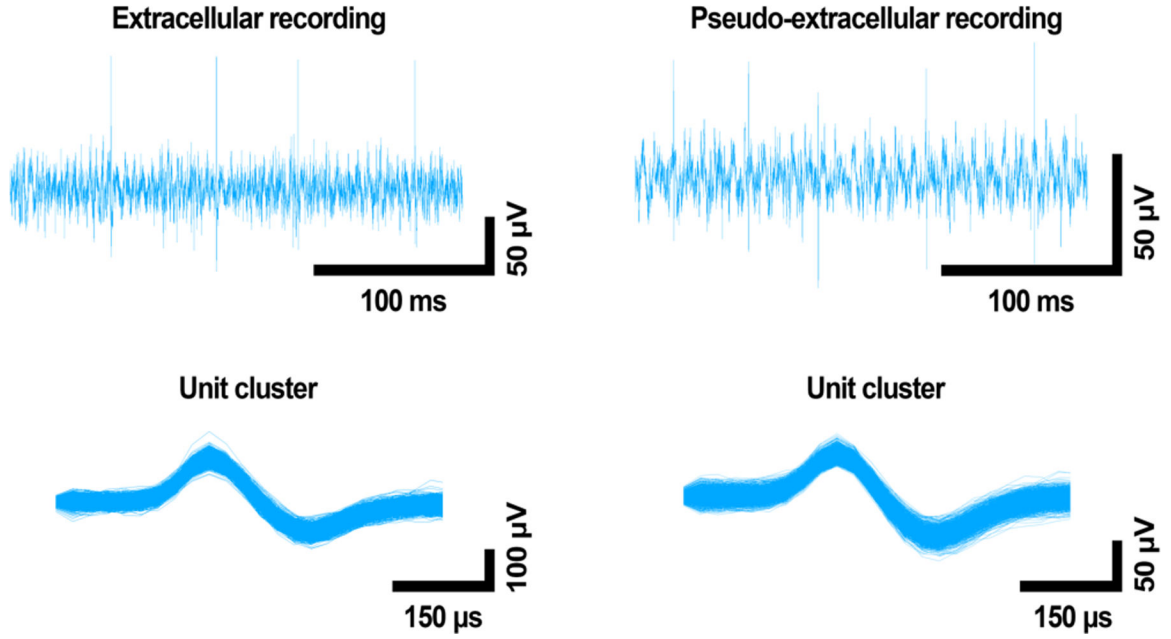


Figure 2: Comparison of the Subject #8 source signal (left) and recorded waveforms (right) in PBS, showing close resemblance of the two. The top row shows high-pass filtered waveforms, and the bottom shows the sorted unit. Voltage is on the y axis, and time on the x axis. “Extracellular recording” refers to the original data acquired *in vivo*; “Pseudo-extracellular recording” refers to data acquired in PBS. Here, only the Subject #8 waveform was applied to the solution.

Subject #10: extracellular recording vs. pseudo-extracellular recording

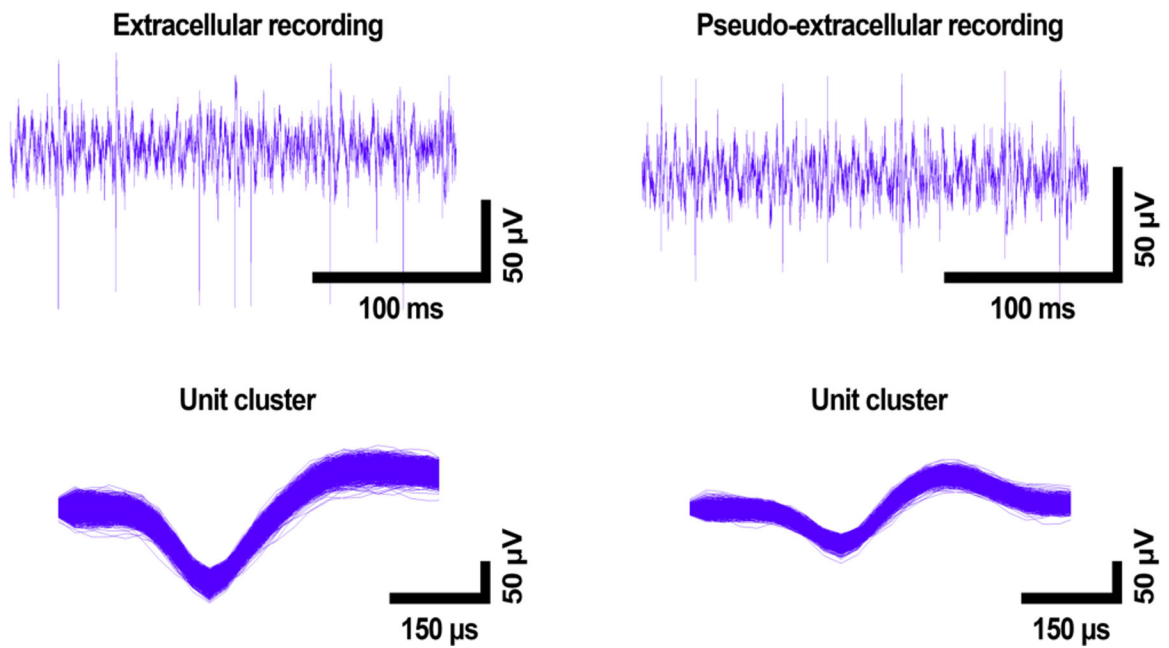


Figure 3:

Comparison of the Subject #10 source signal (left) and recorded waveforms (right) in PBS, showing close resemblance of the two. The top row shows high-pass filtered waveforms, and the bottom row shows the sorted unit. Voltage is on the y axis, and time on the x axis. “Extracellular recording” refers to the original data acquired *in vivo*; “Pseudo-extracellular recording” refers to data acquired in PBS. Here, only the Subject #10 waveform was applied to the solution.

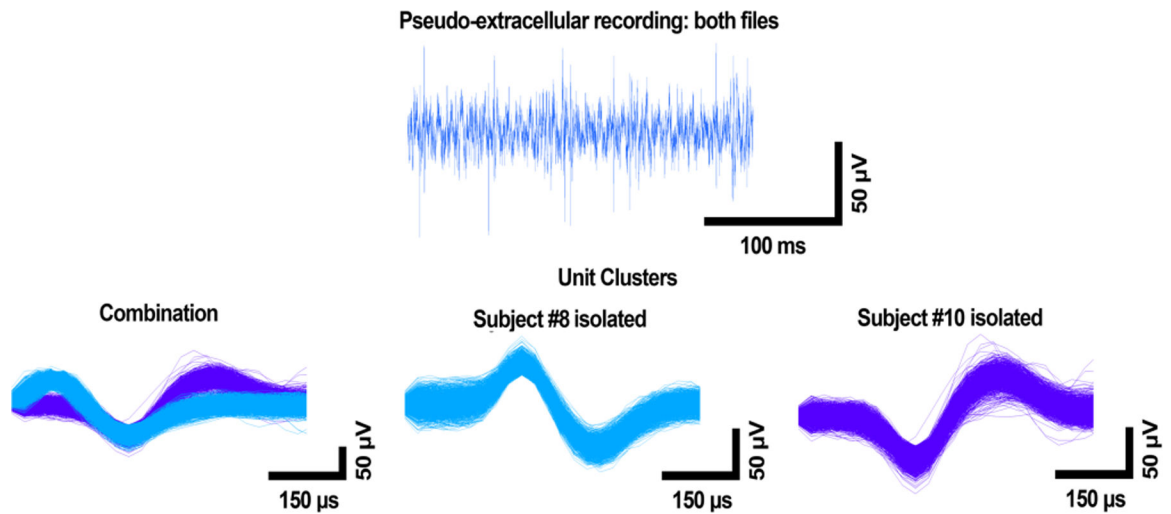


Figure 4:

High-pass filtered waveform and sorted spikes from multi-sound file recording. From left to right, the bottom row shows the waveforms together after alignment and sorting, as well as each unit on its own for clarity. Part of Subject #8's waveform is cut off in the combination figure, as it was necessary to align by global minimum. A more complete waveform for Subject #8 is shown to the right of the combination figure. Voltage is shown on the y axis, and time on the x axis.